Internal Electrostatic Potentials in Bilayers: Measuring and Controlling Dipole Potentials in Lipid Vesicles

J. Craig Franklin and David S. Cafiso
From the Department of Chemistry and Biophysics Program at the University of Virginia, Charlottesville, Virginia 22901 USA

ABSTRACT The binding and translocation rates of hydrophobic cation and anion spin labels were measured in unilamellar vesicle systems formed from phosphatidylcholine. As a result of the membrane dipole potential, the binding and translocation rates for oppositely charged hydrophobic ions are dramatically different. These differences were analyzed using a simple electrostatic model and are consistent with the presence of a dipole potential of approximately 280 mV in phosphatidylcholine. Phloretin, a molecule that reduces the magnitude of the dipole potential, increases the translocation rate of hydrophobic cations, while decreasing the rate for anions. In addition, phloretin decreases the free energy of binding of the cation, while increasing the free energy of binding for the anion. The incorporation of 6-ketocholestanol also produces differential changes in the binding and translocation rates of hydrophobic ions, but in an opposite direction to those produced by phloretin. This is consistent with the view that 6-ketocholestanol increases the magnitude of the membrane dipole potential. A quantitative analysis of the binding and translocation rate changes produced by ketocholestanol and phloretin is well accounted for by a point dipole model that includes a dipole layer due to phloretin or 6-ketocholestanol in the membrane-solution interface. This approach allows dipole potentials to be estimated in membrane vesicle systems and permits predictable, quantitative changes in the magnitude of the internal electrostatic field in membranes. Using phloretin and 6-ketocholestanol, the dipole potential can be altered by over 200 mV in phosphatidylcholine vesicles.

INTRODUCTION

Several distinct electrostatic potentials can be defined in lipid bilayers that arise from a number of sources. For example, transmembrane potentials result from charge separation across the membrane, and membrane surface potentials result from charge that is bound to the membrane-solution interface (1). Transmembrane potentials are known to regulate the activity of certain ion channels, presumably as a result of conformational changes in these proteins that are electrically active. Although they have not yet been characterized, these electrically active structural transitions must involve the movement of protein charges or dipole moments within the membrane interior so that conformational free energies are dependent upon the transmembrane electric field. Surface potentials represent a potential difference between the membrane interface and the bulk aqueous phase. These potentials are usually much smaller than transmembrane potentials, and are typically on the order of a few tens of mV in biological membranes; nonetheless, they appear to have an important role in controlling the binding of charged proteins to membranes. Indeed, surface potentials may control the activity of enzymatic components of second-messenger systems, such as protein kinase C, by regulating the binding of these proteins to the membrane interface (2). In addition to transmembrane and surface potentials, lipid bilayers also possess an internal potential termed a dipole potential. This potential is much larger than either the surface or the transmembrane potentials, and appears to be on the order of 300 mV hydrocarbon positive in phosphatidylcholine vesicles. The existence of the dipole potential has been known for some time, both from electrical measurements in monolayers (3) and work in model bilayers. In bilayers, it is believed to account for the permeability differences of certain organic cations and anions (4–10). Unlike the surface potential, the dipole potential is independent of ionic strength; hence, it is thought to result from oriented dipoles in the membrane interface. The molecular source of the dipole potential has not been clearly identified; however, carbonyl oxygens and/or water at the membrane interface appear to be the most likely sources of this potential. (11–13) A major role for water is suggested by recent electrostatic calculations (14), as well as by an apparent connection between the hydration pressure and the dipole potential (12).

The magnitude of the dipole potential suggests that it should be important in a number of processes. For example, conformational changes in membrane proteins that result in the movement of charge or dipole moments through the membrane interface will be affected by the dipole potential. The insertion of α-helical segments of proteins into membranes should also be modulated by the dipole potential, and this interaction may be an important energetic term affecting the insertion of peptides or signal sequences into membranes (15). The dipole potential is also expected to slow the translocation of positively charged segments of membrane proteins during biosynthesis. As a result, the dipole potential might account for the presence of positively charged residues in stop-transfer sequences (16). Finally, virtually all efficient protonophores are hydrophobic weak acids that shuttle across bilayers in a negatively charged form (17). The lack

Received for publication 9 December 1992 and in final form 12 March 1993.
Address reprint requests to David S. Cafiso.

0006-3495/93/07/289/11 $2.00

of any efficient weak base protonophores is likely the result of the large the dipole potential, since these compounds would need to shuttle charge in a positively charged form.

In spite of its likely importance, the role of the dipole potential in controlling protein interactions with membranes or its affect on membrane protein conformation has not been demonstrated. This is a result of the fact that experimental systems to examine these protein-membrane electrostatic interactions have not been explored. The majority of studies on dipole potentials in membranes have been carried out in planar bilayer systems, and, while these systems provide a facile means to monitor ion conduction, they do not readily permit the measurement of events such as protein binding or the characterization of protein structural changes. However, membrane dipole potentials can also be estimated in lipid vesicles where structural studies on proteins are also possible (10).

An estimate of the dipole potential in vesicles can be made by examining the membrane permeability and binding of certain organic ions termed hydrophobic ions. Shown in Fig. 1 are the calculated free energy profiles for transferring the hydrophobic cation tetraphenylphosphonium, ϕ_4P^+, and the anion, tetraphenylborate ϕ_4B^-, from solution across a lipid bilayer in the absence of a surface potential. This energy is estimated by adding together ΔG_{Born}, the electrostatic Born-Image energy, ΔG_{Hydro} the (attractive) hydrophobic energy, and ΔG_{Dipole} the energy of interaction of the ion with the membrane dipole field (10).

$$\Delta G^o = \Delta G^o_{Born} + \Delta G^o_{Dipole} + \Delta G^o_{Hydro} \quad (1)$$

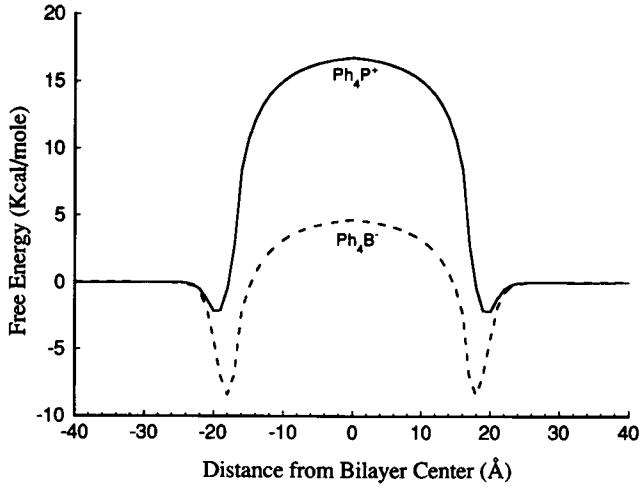

FIGURE 1 Free energy profiles across lipid bilayers for the hydrophobic ions tetraphenylborate (ϕ_4B^-) and tetraphenylphosphonium (ϕ_4P^+). These energy profiles are calculated by adding together terms due to the electrostatic charging or Born-Image energy, the hydrophobic binding energy, and the energy due to the dipole potential. The dipole potential makes these two profiles dramatically different, a feature that accounts for the increased binding and increased translocation rates of ϕ_4B^- when compared to ϕ_4P^+. These profiles were determined as described previously (10), where the intrinsic membrane dipoles have a strength of 0.85 D with the density of the lipid. The magnitude of the neutral binding energy was taken as –6.8 kcal/mol, with an ion radius of 4.2 and 4.0 Å for ϕ_4B^- and ϕ_4P^+, respectively.

The large size of these ions lowers ΔG_{Born}, which makes them quite membrane permeable. As a result of their hydrophobicity, the free energy profiles also show a minimum within the membrane solution interface, and they are experimentally observed to bind to a low dielectric domain of the membrane (11). The differences between energy curves for the hydrophobic cation and anion depicted in Fig. 1 are a direct consequence of the dipole potential. As is readily appreciated from Fig. 1, the dipole potential creates dramatic differences in the translocation and binding of hydrophobic ions, by altering the free energy barrier in the middle of the bilayer and the depth of the free energy minima at the interfaces. In fact, otherwise similar cations and anions are observed experimentally to have as much as a 10^6 times difference in their transport rate constant (18). By modeling the experimental binding and translocation rates of hydrophobic ions, an estimate of the dipole potential is possible.

A number of compounds are known to modify the dipole potential of bilayers. For example, phloretin is a compound that appears to reduce the magnitude of the dipole potential, and it has been studied in planar bilayer systems (19–21). Previous work carried out in this laboratory demonstrated that phloretin produces changes in the translocation rates of hydrophobic ions in lipid vesicles that are consistent with the magnitude of its molecular dipole moment (22). In these vesicle systems the membrane concentration of phloretin can be easily determined, which makes a quantitative evaluation of its action possible. In addition to changes in the translocation rates of hydrophobic ions, changes in the dipole potential should also produce changes in the binding of hydrophobic ions (10), however, these binding changes have not been measured.

Recently, several newly developed spin-labeled hydrophobic anion probes were described that allow the direct measurement of hydrophobic anion transport and binding in vesicle systems (23). These probes provide an excellent complement to previously developed positively charged phosphonium probes (24). In the present study, both the translocation rates and binding free energies of oppositely charged spin-labeled hydrophobic ion probes (**I–III** below) are examined in vesicles. In the context of a simple model, we demonstrate that these probes provide an estimate of the membrane dipole potential. In addition, the effects of phloretin and 6-ketocholestanol on both the binding and transport rates of these probes are examined. Ketocholestanol is an agent that increases monolayer surface potentials, and it is expected to increase the membrane dipole potential (25). The changes produced by these agents on the binding and transport of hydrophobic ions are shown to be consistent with the effects of adding the molecular dipole moment of these molecules to the membrane-solution interface. The use of these compounds allows the dipole potential to be lowered or raised over a wide magnitude and provides an excellent experimental methodology to examine the effects of dipole potentials on membrane protein structure and binding.

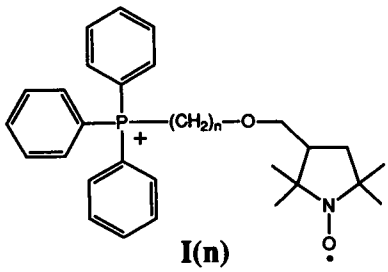

I(n)

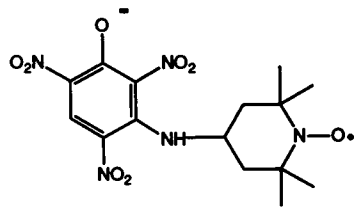

II

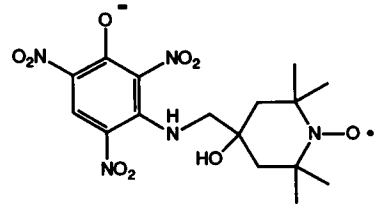

III

SCHEME I–III.

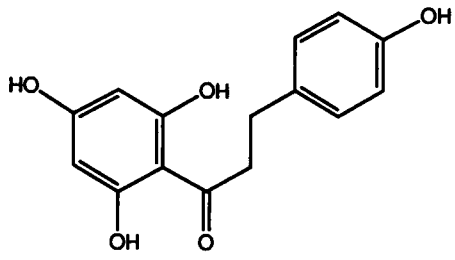

Phloretin

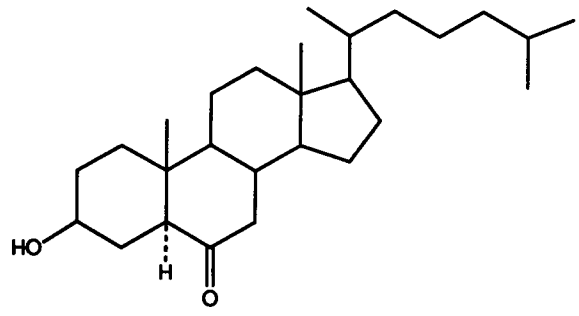

6-ketocholestanol
(5α-cholestan-3βol-6-one)

SCHEMES IV and V.

EXPERIMENTAL PROCEDURES

Materials

Phosphatidylcholine (PC) was isolated from fresh hens eggs using the procedure of Singleton et al. (26) and was stored in a chloroform solution at −20°C until needed. The spin-labeled phosphoniums **I(n)** were synthesized following a procedure described previously except that the appropriate dibromoalkanes were coupled to five membered proxyl nitroxides rather than the six membered TEMPO nitroxide (18). The trinitrophenols **II** and **III** were synthesized using a procedure recently described (22). Phloretin was obtained from Sigma Chemical Co. (St. Louis, MO), and 6-ketocholestanol was obtained from Steraloids (Walton, NH).

Methods

Formation of lipid vesicles

Aliquots of the egg PC solution were dried by rotary evaporation, and varied amounts of 6-ketocholestanol or phloretin were incorporated by codissolving these compounds with the egg PC using benzene/methanol (95:5). The mixtures were then freeze-dried for a minimum of 15 h at less than 0.5 torr. Lipid vesicles were formed by dissolving the dried lipid film with 1 ml of an aqueous solution containing 100 mM NaCl and 25 mM morpholinopropane sulfonic acid (MOPS), pH 7.0. The suspension was vortexed, freeze-thawed five times, and extruded 10 times through 0.05-μm Nucleopore filters using a commercial unit (Lipex Biomembranes Inc., Vancouver, BC). The vesicles were centrifuged at 12,000 *g* to remove nonvesicular lipid. An analysis of both the supernatant and pellet by thin-layer chromatography showed that the lipid and phloretin (or ketocholestanol) were uniformly mixed in each fraction. The phospholipid concentration of the final vesicle suspension was determined using a modified Fiske-Subbarrow phosphate assay (27).

EPR determination of hydrophobic ion binding

EPR measurements were performed on a Bruker ESP 300 EPR spectrometer, and the binding of spin-labeled probes was determined as described previously (24). Briefly, in the presence of lipid vesicles the spin-labeled probes **I–III** partition between the membrane and aqueous phases. The resulting EPR spectrum under these conditions is simply a sum of the spectra produced by membrane associated and aqueous spins. Because the signal intensities are proportional to the number of spins in each phase, a quantitative measure of the resonance intensities can be used to measure the phase partitioning of **I–III**. The ratio of the number of membrane-bound spins to the number of spins in solution, λ, is given by:

$$\lambda = \frac{(A_f^o - A)}{[A - (b/a)A_f^o]} \tag{2}$$

where A is the baseline to peak amplitude of the high-field nitroxide resonance (m = −1) in the lipid suspension, A_f^o is the amplitude of this resonance in the absence of vesicles, and b/a is a constant that reflects the contributions that membrane and aqueous spins make to the amplitude of the $m_I = -1$ resonance (the values of b/a used were 0.04 for probe **I** and 0 for probes **II** and **III**).

As described previously (18) the phase partitioning, λ, of hydrophobic ions such as **I–III** is related to the partition coefficient β, the concentration of lipid C_L, the area/lipid, A_L, and the volume/mole of lipid, V_L, by the following.

$$\frac{1}{C_L} = \beta A_L \frac{1}{\lambda} + V_L \tag{3}$$

A plot of λ^{-1} versus C_L is expected to yield a straight line with a slope of β. The values of A_L and V_L used here were 66 Å^2 and 1255 Å^3, respectively. The binding constant, K, is determined by dividing the partition coefficient

by the thickness of the binding domain for the hydrophobic ion at the vesicle surface. For the hydrophobic ion probes used here this distance is taken as 4 Å (18).

EPR determination of hydrophobic ion currents and rate constants

The transmembrane currents for **I** or **III** were determined by mixing solutions of **I** or **III** (final concentrations were approximately 20 μM) with the egg PC vesicle suspensions. This was accomplished using a precision mixing ram (model 715; Update Instrument, Inc., Madison, WI) adapted to a quartz flat cell in a standard X-band cavity. Upon mixing, a time-dependent change in the amplitude of the high-field resonance of probe **I** or **III** occurs which is a direct consequence of the transmembrane migration of the probe (28). This decrease in amplitude (increase in membrane binding) is due to the increase in accessible membrane surface area that accompanies probe equilibration with the internal vesicle surface. The signal intensity A can be related to the transmembrane ion current by:

$$i = -\frac{bzF}{S_o}\left[\frac{K_o V_{mo}/V_o}{1 - \epsilon_o/\epsilon_i}\right]\left[\frac{dA}{dt}\right] \quad (4)$$

where S_o is the external vesicle surface area, K_o and K_i are the external and internal probe binding constants, V_{mo} and V_{mi} are the external and internal volumes occupied by the probe, respectively, $\epsilon_o = (1 + K_o V_{mo}/V_o)$, and $\epsilon_i = (1 + K_i V_{mi}/V_i)$. Equation 3 yields a current for the spin-probes **I** or **III** as a function of the time derivative of the high-field resonance amplitude, dA/dt. If the initial ion current, i_o, is determined from the initial rate of change in the signal intensity, $(dA/dt)_{t=0}$, then the rate constant for inward movement of the label can be calculated according to the following.

$$i_o = \frac{k_f F K_o V_{mo}[I_o]}{S_o} \quad (5)$$

Here, $[I_o]$ is the external aqueous concentration of probe **I** or **III**. A detailed discussion and derivation of these expressions was given previously (28).

Modeling dipole potential changes

The effects of phloretin and 6-ketocholestanol on the binding and transport properties of hydrophobic ion probes were analyzed by employing a total potential model for hydrophobic ions similar to one described previously (10). In this model, point dipoles that generate the intrinsic dipole field of the membrane are placed on a square lattice at a defined distance from the bilayer center. The energy of an ion at any point is taken by calculating the sum of the electrostatic interactions between a charge and the dipole lattice, ΔG_{Dipole}, and adding energy terms for the Born-Image energy, ΔG_{Born}, as well as the neutral (or hydrophobic) energy, ΔG_{Hydro}. An energy profile is obtained by calculating the energy along a path normal to the bilayer surface. This model was modified in two ways for the present study. First, binding and translocation rate data in the absence of phloretin or 6-ketocholestanol were obtained for the hydrophobic ion probes **I**–**III**. This data was combined with previous data on hydrophobic ions, and the parameters in the model were optimized as detailed previously to produce the best fit to the experimentally determined values of k_f and K (10). As discussed below, this yielded slightly different but physically reasonable parameters. Second, as depicted in Fig. 2, the addition of phloretin or 6-ketocholestanol was treated as being equivalent to the addition of dipoles to the membrane interface that were either aligned with or against the intrinsic membrane dipole. This was modeled by placing an additional layer of point dipoles on a second square lattice at a frequency corresponding to the membrane-bound concentration of these compounds (22). Both the magnitude and the position of this additional layer of dipoles was allowed to vary. In the case of phloretin, the dielectric constant of the membrane interior was altered as a function of the phloretin concentration. Phloretin is known to change the capacitance of lipid bilayers, a change that could be due either to a change in membrane dielectric or bilayer thickness (21). Recent ^{2}H NMR work provides no evidence for a change in bilayer thickness in the presence of phloretin (29);

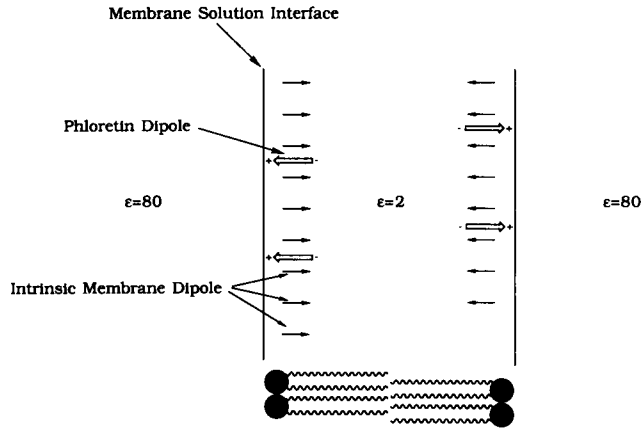

FIGURE 2 A depiction of how phloretin is believed to modify the internal dipole potential of membranes. When phloretin is added to membranes, it inserts into the membrane solution interface and is positioned so that a component of its molecular dipole (approximately 5 D) is aligned against the intrinsic membrane dipoles. The effect of phloretin on hydrophobic ion transport and binding is modeled by calculating the electrostatic energy due to point dipoles on a square lattice at a density corresponding to the membrane concentration of phloretin. The effects of 6-ketocholestanol are modeled in the same manner, except that a component of its molecular dipole adds to the to the intrinsic membrane dipoles.

as a result, the most likely source of this capacitance change is a change in membrane dielectric. In the modeling carried out here, the dielectric constant was varied linearly with the addition of phloretin as given by $\epsilon = 2.0 + x$, where x is the mole fraction of phloretin in the membrane.

This electrostatic model produces a free energy profile for hydrophobic ions in membranes. To compare the measured translocation rates with the predictions of this model, the binding constants and rate constants were calculated from the energy profile in a manner similar to that described previously (10). Briefly, the rate constants, k_f, were calculated from the potential energy profiles of hydrophobic ions by taking the energy difference between the minima at the membrane interface and center of the membrane ($\Delta G^{o\ddagger}$). The rate constant, k_f, was determined from the expression: $k_f = f\exp(\Delta G^{o\ddagger}/RT)$, where f is a universal frequency factor of 6×10^{12} s^{-1} at room temperature (30). The predicted binding constants, K, were determined from the free energy profiles by taking the energy difference between the bulk solution and the minima at the interface (ΔG^{o}_{B}). This energy difference is related to the binding constant by the familiar expression $K = \exp(-\Delta G^{o}_{B}/RT)$.

RESULTS

Phloretin increases the binding of cation probes and decreases the binding of anion probes

The membrane-aqueous phase partitioning of probes **I**–**III** to 500-Å egg PC vesicles can be determined directly from their EPR spectra as described under Experimental Procedures. Shown in Fig. 3 is a plot of the ratio of the number of aqueous to bound spins ($1/\lambda$) for the hydrophobic anion probe **III** plotted versus the reciprocal of the lipid concentration ($1/C_L$). The slope of this curve is linear over the probe concentration shown in Fig. 3 up to a probe:lipid ratio of about 1:100; however, the slope increases at higher probe:lipid ratios. This is consistent with previous data obtained for ϕ_4P^+ indicating that these hydrophobic ions experience an electrostatic saturation in the lipid bilayer at probe:phospholipid

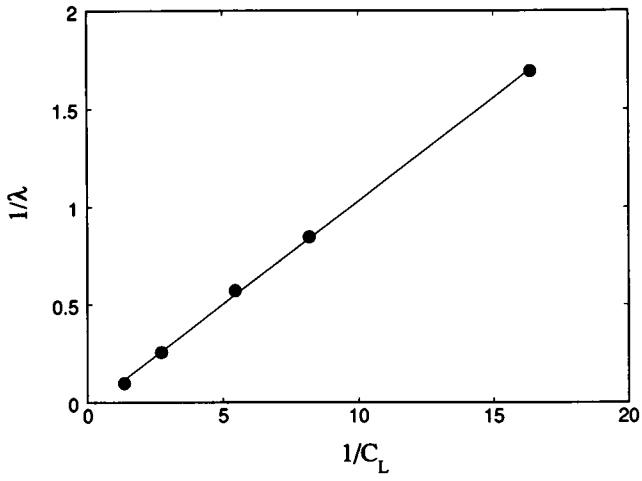

FIGURE 3 A plot of the reciprocal of the partitioning ($1/\lambda$) of **III** versus the reciprocal of the lipid concentration ($1/C_L$, in cm^3 mol^{-1}). The lipid vesicles were formed by extrusion through 0.05-μM Nucleopore filters in a buffer containing 100 mM NaCl and 25 mM MOPS, pH 7.0, and the partitioning of **III** was measured by EPR spectroscopy using procedures described previously (22). The solid line represents a fit of Eq. 2 to the data using a value for the area/lipid, A_L, of 66 $Å^2$ and a value for V_L of 1255 $Å^3$. This fit yields at value for β of 22.4×10^{-5} cm.

ratios above 1:100 (18). From the linear portion of this curve, the partition coefficients, β, were determined for probes **I–III**, and these values of β are shown in Table 1. Inspection of this data shows that the binding of the negatively charged trinitrophenol probes **II** and **III** is clearly stronger than for the positive phosphonium **I**(8), even though the phosphonium probe has significantly more hydrophobic character. As explained above, this difference in binding is a direct consequence of the dipole potential. There are strong indications that the TNP probe **III** is hydrogen-bonded in the membrane interface. First, the hydroxyl group on **III** raises the energy of binding by about 1 kcal/mol compared to probe **II**. This energy difference is much less than the energy loss that would have been expected if this probe were not hydrogen-bonded within the interface. Second, previous work that compared the motion of the two anion probes (**II** and **III**) indicates that the rotational rate of **III** in the bilayer is much slower than that of **II**, consistent with **III** forming a hydrogen bond within the interface (23).

When phloretin is incorporated into the membranes of the 500-Å vesicles the binding of both negative and positively charged hydrophobic ions is altered. Table 1 shows the effect on the partition coefficients of these probes following the incorporation of 5 and 10 mol% phloretin into the membrane. The addition of phloretin produces small but measurable increases in the binding for the positive probe **I**, and two- to threefold decreases in the binding of the hydrophobic anion probes **II** and **III**.

Phloretin increases the crossing rate for cations but reduces the rate for anions

Shown in Fig. 4 is a recording of the high-field resonance of the nitrophenol probe **III** when the probe is mixed with phospholipid vesicles. A similar decay in the high-field resonance amplitude upon mixing with vesicles is seen for phosphonium spin labels such as **I**. These probes rapidly equilibrate with the external vesicle surface, and this decay was previously shown to be the result of the transmembrane migration of the hydrophobic ion (28). From a measure of the time dependence of the EPR signal amplitude, dA/dt, the hydrophobic ion current and translocation rate constant were estimated using Eqs. 3 and 4. Shown in Table 1 are the forward translocation rate constants, k_f, for probes **I** and **III** in vesicles formed from egg PC. The value of k_f for **III** is considerably slower than values obtained previously for the carbonylcyanide *m*-chlorophenylhydrazone (CCCP) anion (22), and is much slower than the crossing rate for probe **II**. In fact, a value of k_f for probe **II** could not be measured, because its transmembrane equilibration is faster than can be resolved with the present instrumentation (<10 ms). This dramatic difference in crossing rates between **III** and other hydrophobic anions such as **II** and CCCP is accounted for by the additional energy that would be required to break a hydrogen bond, consistent with the idea that **III** hydrogen bonds within the membrane interface.

The incorporation of phloretin into the vesicle membrane alters the transport rates of hydrophobic ions. The transport rates for probes **I** and **III**, as well as previous data obtained for the CCCP anion in vesicles, are shown in Table 1 for membranes at two phloretin concentrations. The rate of crossing for the phosphonium **I** is increased approximately 70-fold upon the addition of 10 mol% phloretin, while the crossing rates of the anions are decreased by more modest levels.

Any number of physical changes might be expected to increase the binding of probe I; for example, an increase in the dielectric constant or disordering of the membrane interface. However, the differential effects of phloretin on the

TABLE 1 Effect of phloretin on hydrophobic ion binding and translocation rate constants

	$\beta \times 10^5$ (cm)			$k_f \times 10^3$ (s^{-1})		
Phloretin*	I(8)	II	III	I(4)	CCCP‡	III
0	6.4 ± 1.0	161	22.4	1.39	6000	4.1 ± 1.2
5	8.7	110	14.3	5.0	2400	3.1
10	10.0	65.0	8.15	103	360	1.6

* Approximate phloretin concentration in mol%.
‡ Data from Ref. 22.

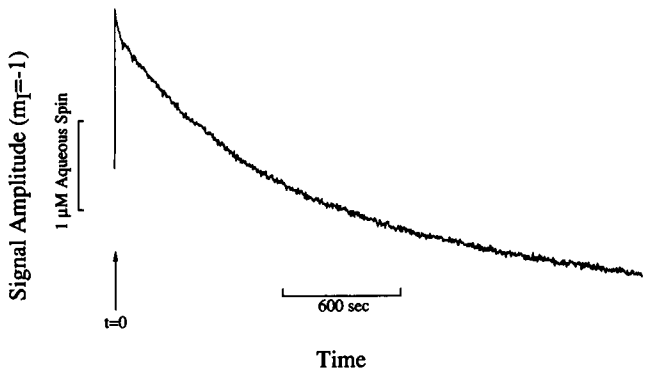

FIGURE 4 A recording of the high-field resonance amplitude ($m_I = -1$) of **III** following mixing with extruded egg PC vesicles. Probe **III** and lipid are mixed to final concentrations of 20 μM and 2 mM in a quartz EPR cell using a precision mixing ram. The decrease in the amplitude of **III** with time is a result of an increase in the membrane partitioning of the probe that accompanies its transmembrane migration. This time-dependent partitioning change is used to estimate the rate constant for the transmembrane migration of **III** (see Experimental Procedures).

binding of oppositely charged probes provides a strong argument that the binding changes are electrical in origin. The fact that phloretin produces opposite effects on the membrane crossing rates of hydrophobic anions and cations, also supports this contention. Both these observations are consistent with a reduction in the magnitude of the dipole potential by phloretin. These phloretin-induced changes in ion translocation rates and binding are analyzed below using a simple electrostatic model.

6-Ketocholestanol produces opposite effects from those of phloretin on hydrophobic ion binding and translocation rate constants

The transmembrane migration rates and binding of probes **I** and **III** were measured in 500-Å extruded vesicles in a manner identical to that for vesicles containing phloretin, except that the vesicle membranes contained 6-ketocholestanol. As shown in Table 2, the incorporation of 6-ketocholestanol decreases both the binding and translocation rate constants of probe **I**, but produces an increase in the binding and crossing rates for the anion probe **III**. This differential behavior in both the binding and transport of oppositely charged probes provides strong evidence that the changes produced are electrostatic in origin. However, the changes produced by 6-ketocholestanol are in an opposite direction and smaller in magnitude than those produced by phloretin. The effects of 6-ketocholestanol on the binding and translocation rates of hydrophobic ions are those expected from an increase in the membrane dipole potential.

TABLE 2 Effect of 6-ketocholestanol on hydrophobic ion binding and translocation rate constants

	$\beta \times 10^5$ (cm)		$k_f \times 10^3$ (s^{-1})	
6K Chol.*	I(8)	III	I(8)	III
0	7.0 ± 1.2	21.8 ± 2	15.7	2.11 ± 0.5
5	5.4	24.1	13.0	6.27
10	4.9	25.0	9.3	7.03

* Approximate concentration of 6-ketocholestanol (6Kchol) in mol%. The values for β and k_f in the absence of 6Kchol are close but not identical to the values shown in Table 1 in the absence of phloretin. These data were obtained using different preparations of egg PC. Values measured using any one preparation of lipid exhibit a variability of approximately 5%; however, when measurements between lipid preparations are compared significant variability is often seen. This is likely a result of the variation in acyl chain heterogeneity between these preparations.

A simple electrostatic model can account for the effects of phloretin and 6-ketocholestanol on hydrophobic ion binding and translocation

The data presented in Tables 1 and 2 are qualitatively consistent with a lowering and raising of the membrane dipole potential by phloretin and 6-ketocholestanol, respectively. To determine whether these changes are quantitatively consistent with a change in dipole potential, the experimental rates were compared with the predictions of a simple electrostatic model. This model can be used to generate a free-energy profile for hydrophobic ions, and it was previously shown to account for the binding and translocation rates of the hydrophobic ions ϕ_4P^+ and ϕ_4B^- (10). This model also provides a mechanism for estimating the magnitude of dipole potential changes produced by phloretin and 6-ketocholestanol.

As described under Experimental Procedures, physically realistic parameters were determined for this model by fitting the binding and translocation data for the hydrophobic ions **I**, **II**, and **III** as well as data previously obtained for ϕ_4B^- and ϕ_4P^+ (in the absence of phloretin or 6-ketocholestanol). The predictions of this model for the binding and activation energies of hydrophobic ions in egg PC vesicles are given in Table 3. Table 3 also provides a comparison of the measured and calculated data for the hydrophobic ions. The parameters that were used in this model are given in the legend to Table 3. As is readily apparent, the agreement between the measured and modeled values of K and k_f is excellent. Compared

TABLE 3 Hydrophobic ion binding and translocation free energies in kcal/mol

Ion	$\Delta G_{B(measured)}$	$\Delta G_{B(model)}$	$\Delta G‡_{(measured)}$	$\Delta G‡_{(model)}$
ϕ_4P^+	−2.8	−2.9	19.7	20.2
ϕ_4B^-	−7.5	−7.45	13.5	11.76
I(8)	−4.4	−4.5	19.5	20.7
III	−5.1	−5.08	18.9	17.9
II	−6.1	−6.4		12.7

The measured values for ΔG^o and $\Delta G^o‡$ were calculated as described under Experimental Procedures using a point dipole model described previously (10). The neutral binding energies used in this calculation for ϕ_4P^+, ϕ_4B^-, I(8), II, and III were −6.8, −6.8, −8.8, −4.6, and −4.6 kcal/mol, respectively. The ionic radii for ϕ_4P^+, ϕ_4B^-, I(8), II, and III used were 4.2, 4.0, 4.0, 3.75, and 3.75 Å, respectively, and the dipole layer was placed at a position 19 Å from the bilayer center. Because probe **III** appears to hydrogen bond in the membrane interface, an additional 5 kcal/mol was added for the transfer of this group from the interface into the membrane interior.

with the previous calculation of hydrophobic ion energies (10), the present modeling places the intrinsic dipole layer deeper in the interface (approximately 19 Å from the membrane center), and it produces a better fit with the experimental values of K and k_f for ϕ_4P^+ and ϕ_4B^-. Using this point dipole model, it is possible to estimate the magnitude of the membrane dipole potential. With the parameters that produce the values shown in Table 3, the membrane dipole potential is estimated to be 280 mV in egg PC vesicles.

To account for the effect of adding phloretin or 6-ketocholestanol an additional dipole lattice was included into the dipole energy calculation (as described under Experimental Procedures). Thus, the effect of these agents is treated strictly as the result of an additional electrostatic field due to their intrinsic dipole moments. Using the model and parameters that produced the values shown in Table 3, the magnitude and position of dipoles in this second lattice were varied until the best fit with the experimental data was found. In each case a best fit occurred when the position of the added dipole layer coincided with the position of the intrinsic dipole layer. Shown in Fig. 5 *A* is a plot of the ratio k_f/k_f^o for oppositely charged spin probes as a function of the phloretin concentration, where k_f and k_f^o are the forward rate constants in the presence and absence of phloretin, respectively. The plot in Fig. 5 *B* shows the ratio of the binding constants K/K^o for oppositely charged probes as a function of the phloretin concentration, where K and K^o are the binding constants in the presence and absence of phloretin. In both figures the solid lines represent the predictions of the point dipole model. The agreement between the experimental and predicted K and k_f values is quite good, and indicates that this simple model can account for the effects of phloretin on the binding and translocation rates of these ions. These solid lines correspond to the case where phloretin is adding an effective molecular dipole of approximately 2.2 Debye (D) antiparallel to the intrinsic dipole moment of the bilayer. Both the model and the experimental data reveal an asymmetry in the effect of phloretin on hydrophobic cations and anions, a feature that will be discussed below.

The effect of 6-ketocholestanol on the binding and rate constants for the hydrophobic ion probes **I** and **III** was analyzed in an identical manner to that shown for phloretin, and the results are shown in Fig. 6, *A* and *B*. The solid lines again represent the best fits of the simple dipole model to the experimental values of k_f/k_f^o and K/K^o as a function of the 6-ketocholestanol concentration. Within experimental error the behavior of the positively charged phosphonium (as a function of 6-ketocholestanol concentration) is accurately predicted by the model. The behavior of the negatively charged TNP probe **III** is not as accurately predicted, although the largest energy differences between the calculated and measured values of K and k_f are small (<0.4 kcal/mol). The effective molecular dipole used to calculate the solid lines in Fig. 6 is 1 D aligned in a direction parallel to the intrinsic molecular dipole. Thus, 6-ketocholestanol acts to increase the magnitude of the membrane dipole potential,

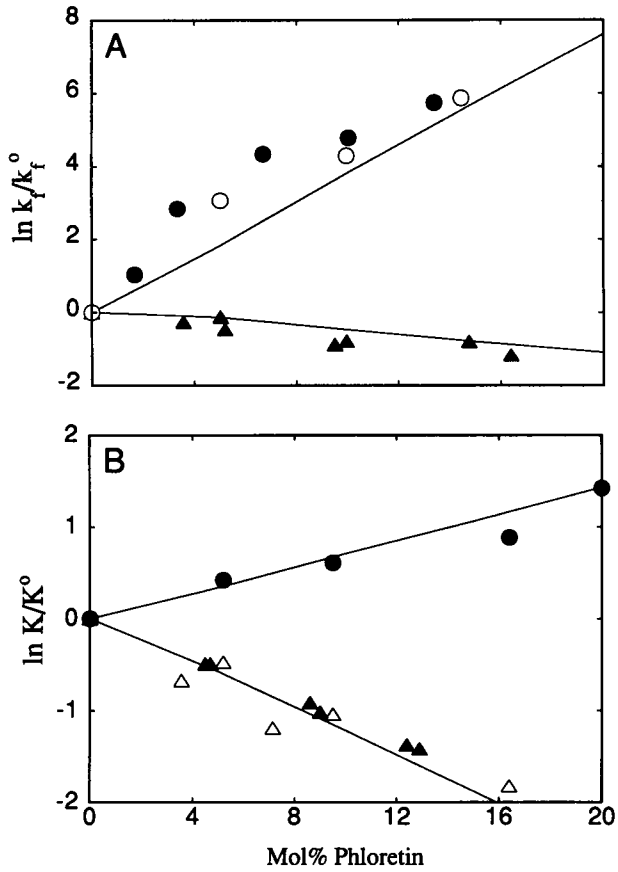

FIGURE 5 Experimental and predicted effect of phloretin on the rate constants and binding constants of hydrophobic ions in PC membranes. (*A*) A log plot of the ratio of transmembrane kinetic rate constants, k_f/k_f^o, where k_f and k_f^o are the rate constants in the presence and absence of phloretin, respectively. Experimental data are shown for (○) probe **I**(4), (●) probe **I**(4) taken from Ref. 20, and (▲) probe **III**. (*B*) A log plot of the ratio of binding constants, K/K^o, where K and K^o are the binding constants in the presence and absence of phloretin, respectively. Experimental data are shown for (○) probe **I**(8), (▲) probe **II**, and (△) probe **III**. For both *A* and *B*, the solid lines represent the predictions of a point dipole model where phloretin inserts a dipole of 2.2 D at a distance of 19 Å from the bilayer center (see Experimental Procedures).

and it is less than half as effective at producing absolute changes in this potential compared to phloretin.

The intrinsic dipole moments of phloretin and 6-ketocholestanol

To determine whether the intrinsic dipole moments of phloretin and 6-ketocholestanol are consistent with the changes they produce in the membrane dipole potential, their energy-minimized structures and dipole moments were calculated using version 6 of MOPAC. These dipole moments and structures are shown in Fig. 7. The dipole moment of 6-ketocholestanol is approximately 3.1 D, and the positive end of the dipole is oriented so that makes an angle of about 40° with respect to the axis of the sterol ring system (defined by a line between carbons 1 and 12 in the ring system). Since this axis is expected to lie roughly along the bilayer normal,

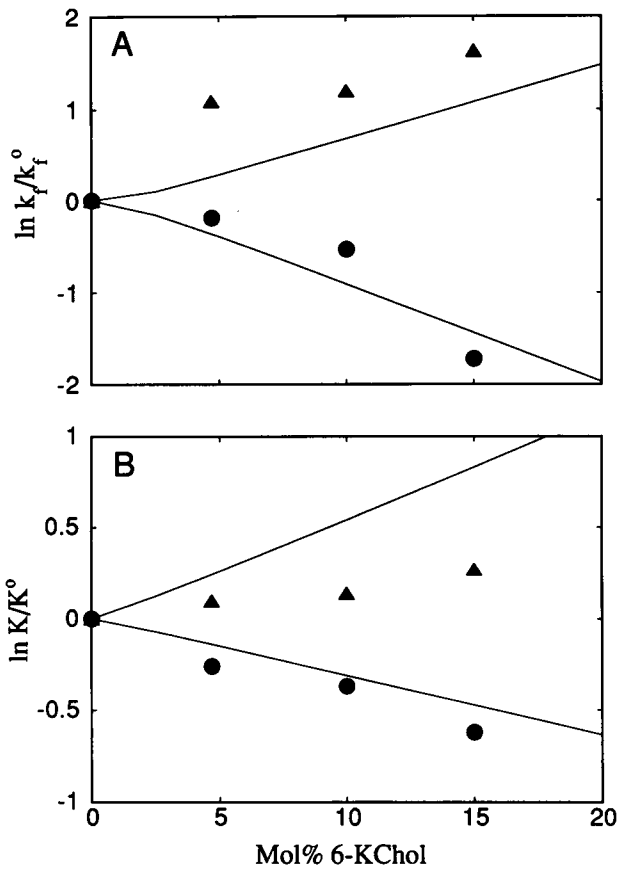

FIGURE 6 Experimental and predicted effect of 6-ketocholestanol on the rate constants and binding constants of hydrophobic ions in PC membranes. (*A*) A log plot of the ratio of transmembrane kinetic rate constants, k_f/k_f^o, where k_f and k_f^o are the rate constants in the presence and absence of 6-ketocholestanol, respectively. (*B*) A log plot of the ratio of binding constants, K/K^o, where K and K^o are the binding constants in the presence and absence of 6-ketocholestanol, respectively. For both *A* and *B*, experimental data are shown for (●) probe **I**(8) and (▲) probe **III**. The solid lines represent the predictions of a point dipole model where 6-ketocholestanol inserts a dipole of 1 D at a distance of 19 Å from the bilayer center (see Experimental Procedures).

the dipole moment should be in a direction that adds to the intrinsic dipole potential of the bilayer. This is consistent with the experimental increase in the dipole potential produced by 6-ketocholestanol. If the bilayer normal is rigorously taken to be along the axis shown in Fig. 7 *A*, this compound should add an effective dipole moment of about 2.4 D. The effective dipole added by ketocholestanol is about half this value, which could be a result of any number of effects. These effects could include small changes in the structure of the interface produced by its addition or a different membrane orientation than that depicted in Fig. 7.

The dipole moment of phloretin determined by MOPAC is 4.2 D, slightly less than the experimentally reported dipole moment of 5 D (21). The direction of this dipole moment with respect to the axis of the trihydroxyphenyl ring is about 109° (see Fig. 7 *B*). Because the trihydroxyphenyl ring of phloretin is expected to be oriented toward the surface of the bilayer, the dipole moment for this molecule should produce a component antiparallel to the intrinsic dipole of the membrane. This picture is qualitatively consistent with the data presented above, although a quantitative evaluation of the effect of phloretin is complicated by the fact that its membrane orientation and structure are not known.

This analysis clearly ignores more complicated interactions that may occur with phloretin or 6-ketocholestanol in the membrane (for example, effects on the water or carbonyl oxygens at the interface). Nonetheless, it does indicate that the direction of the molecular dipole moments of these molecules, taken together with their likely orientations in the membrane, are qualitatively consistent with the experimentally observed changes in hydrophobic ion binding and transport observed here.

DISCUSSION

When hydrophobic anions and cations are compared, they are found to exhibit dramatically different binding energies and rates of membrane transport. These differences are consistent with the presence of a huge internal dipole potential in bilayers (8). Other evidence for the existence of a large internal electrostatic potential has been obtained from measurements of monolayer surface potentials (3), and the complex morphologies of PC monolayer phases (31). The dipole potential arises from dipolar groups in the membrane interface, and its effect on hydrophobic ion binding and transport can be accounted for by a simple electrostatic model (10). The work presented here examined the effects of agents that modify this internal dipole potential on the transport and binding of hydrophobic ions in lipid vesicles. When incorporated into vesicle membranes, phloretin and 6-ketocholestanol change the behavior of hydrophobic ions in a manner that is consistent with a lowering and raising of the dipole potential, respectively.

There are several important reasons to characterize dipole potential changes in vesicle systems. First, the membrane composition and the binding of hydrophobic cations can be well-characterized in vesicle systems. This allows for a quantitative evaluation of the effects of compounds such as phloretin and 6-ketocholestanol, and permits an evaluation of the mechanisms by which they act. Second, procedures to modulate dipole potentials in vesicles provide the basis for an experimental system that can be used to examine the effects of membrane electrostatics on membrane proteins. Vesicle systems are accessible to numerous spectroscopic and biochemical methods; as a result, measurements in vesicles permit a characterization of the conformation, activity, and membrane binding of proteins or peptides as a function of the dipole potential.

The measurements made here provide strong evidence that the changes in ion binding and transport produced by phloretin and 6-ketocholestanol are electrostatic in origin. Conceivably, the addition of phloretin could produce nonelectrostatic changes in the lipid bilayer that might affect the behavior of hydrophobic ions. For example, phloretin might produce changes in the lipid acyl chain packing, or interact

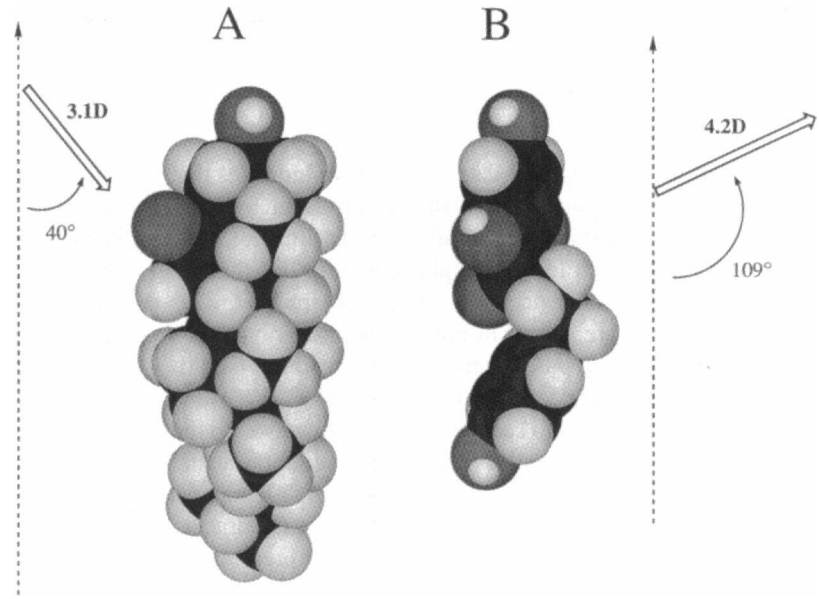

FIGURE 7 Energy minimized structures and dipole moments for (*A*) 6-ketocholestanol and (*B*) phloretin obtained from MOPAC, version 6. The axis in *A* is drawn parallel to the line defined by carbons 1 and 12 of the sterol ring system. The dipole moment of 6-ketocholestanol is oriented at an angle of approximately 40° with respect to this axis as shown. This axis should be roughly parallel to the bilayer normal, and would place the positive end of the ketocholestanol dipole toward the membrane interior. The axis in *B* is defined by a line through the trihydoxylated aromatic ring of phloretin, and the dipole moment of phloretin makes an angle of 109° with respect to this axis.

specifically with the probes **I–III**. Several observations argue against a significant role for these nonelectrostatic effects. First, both phloretin and 6-ketocholestanol produce opposite effects when cations and anions are compared. If these effects are not due to electrostatics, a complicated process would be needed to explain them. Second, the experimental data is reasonably well accounted for by a simple model that treats the effects of phloretin or 6-ketocholestanol strictly as the result of electrostatics. Finally, these agents do not produce dramatic changes in bilayer structure or dynamics. Previous work using ^{2}H NMR found no evidence that phloretin significantly alters the acyl chain order or lipid packing of the membrane (29). Unlike cholesterol, 6-ketocholestanol does not appreciably modify the bilayer thickness and produces a much smaller increase in the compressibility modulus of bilayers than does cholesterol (25). Using ^{2}H NMR, 6-ketocholestanol also produces much smaller changes in acyl chain order than does cholesterol (Franklin and Cafiso, unpublished observation).

The method that was used here to model the transport and binding of hydrophobic ions accurately predicts the binding energies and transport rates of a wide range of hydrophobic ions. This approach made use of a simple dielectric model for the membrane similar to one used previously (10). A number of the parameters used in this model differed slightly from those used in the original model (see Table 3). For example, the intrinsic dipole layer was placed deeper into the membrane interface at a position 19 Å from the bilayer center. This position provided the best fit with the experimental binding constants and rates for a range of hydrophobic ions. This is a physically reasonable position for the dipole layer. Based on previous NMR and EPR studies, the region that gives rise to the dipole potential appears to be near the carbonyl oxygens (and close to the hydrocarbon water interface) (11, 32). In palmitoyloleoyl PC membranes, the carbonyl oxygens reside at approximately 19 Å from the membrane center (25). The value used for the neutral binding energy of ϕ_4B^- or ϕ_4P^+ was also different from that used in the original model. This value was −6.8 kcal/mol and is within the range of energies expected for these ions.

Once the parameters in this electrostatic model were chosen, the effects of phloretin or 6-ketocholestanol were modeled simply by adding in an additional dipole layer to the membrane interface. The effects of phloretin or 6-ketocholestanol were fit best when the added dipole layer coincided with the location of the intrinsic dipole layer, suggesting that these agents act by placing their molecular dipole at the level of the carbonyl oxygens. In spite of the simplifications inherent in this model, the effects of phloretin and 6-ketocholestanol could be reasonably well reproduced. This model clearly ignores any effects of these agents on hydrophobic ions that are due to nonelectrostatic interactions. As shown in Fig. 6, the binding of the TNP probe **III** is underestimated by the model in the presence of 6-ketocholestanol, while the effect of 6-ketocholestanol on the transport rate is overestimated. This indicates that the energy of the TNP probe is slightly higher in the interface in the presence of 6-ketocholestanol than predicted based on the electrostatic model. This energy difference is small and is only 300 cal/mol at 15 mol% 6-ketocholestanol. Conceivably, the small bilayer structural changes that are observed to occur with ketocholestanol addition might account for this discrepancy (25).

As seen in Figs. 5, *A* and *B*, the effects on ion binding and translocation with phloretin are asymmetric. Phloretin has a greater effect on the binding of anions than cations, and a larger effect on the translocation rate of cations compared to anions. This is a result of two features in the model. As pointed out previously (22), hydrophobic cations and anions have slightly different binding positions in the interface and will therefore sense a different fraction of the field due to an added dipole layer. Second, as described above, the addition

of phloretin produces a change in the dielectric constant of the membrane, a feature that tends to accelerate the crossing rates for both anions and cations.

One purpose of the present study was to establish a methodology that could be used to produce changes in the dipole potential of membranes. The data given above indicates that the changes in the dipole potential that are produced by phloretin and ketocholestanol are significant. To illustrate this point, free energy profiles for the phosphonium I(8) that are expected in the presence of 15 mol% phloretin or 6-ketocholestanol are shown in Fig. 8. These energy curves were calculated using parameters that produced the best fit to the experimental data given in Figs. 5 and 6. From this energy profile, it is easy to see that phloretin lowers both the barrier to transport, as well as the binding minima at the membrane solution interface. The addition of 6-ketocholestanol produces an opposite effect that is not as large in magnitude. The energy barrier is shifted in the presence of 15 mol% phloretin versus 6-ketocholestanol by about 5 kcal/mol or approximately 220 mV in egg PC vesicles. This represents a substantial change in the internal potential of the membranes, one that might affect the binding of certain of peptides or the operation of membrane proteins.

In general, monolayer measurements yield higher estimates of the dipole potential compared to measurements in bilayers by 100–150 mV (12), and the measurements made here are no exception. The value found for egg PC is about 280 mV, considerably less than the 400-mV potential usually reported for phosphatidylcholine monolayers. At the present time, the reason for this difference is not understood. Vesicle and bilayer measurements make use of molecular probes, and it has been suggested that these probes might be the source of this discrepancy (12). While problems can be imagined because of the use of probes, a wide range of measurements demonstrate that the probes used here quantitatively respond to transmembrane and surface electric fields (23, 24, 28). In addition, the behavior of several different types of hydrophobic ion probes is found to be consistent with the dipole potentials measured here. When monolayer surface potentials are plotted versus the monolayer area, the measured potentials do not intersect the ordinate at zero potential. It has been noted that the extrapolated surface potential at the ordinate, ΔV_o, is approximately the difference between the monolayer and bilayer measurements (3). Thus, these measurements might contain an additional potential component due to the reorganization of the interface upon formation of the monolayer. It should also be noted that monolayer potentials have been measured for membranes containing equimolar concentrations of PC and 6-ketocholestanol (25). The potential of these membranes is found to be larger by about 300 mV compared to pure PC membranes. The changes in ion binding and translocation rate seen here in PC membranes containing 15 mol% 6-ketocholestanol correspond to a dipole potential increase of about 50 mV. Thus, the two measurements are qualitatively consistent. However, the estimate of the dipole potential change in vesicles is about half that seen in monolayer systems, assuming a linear relationship between the concentration of 6-ketocholestanol and the change in the dipole potential.

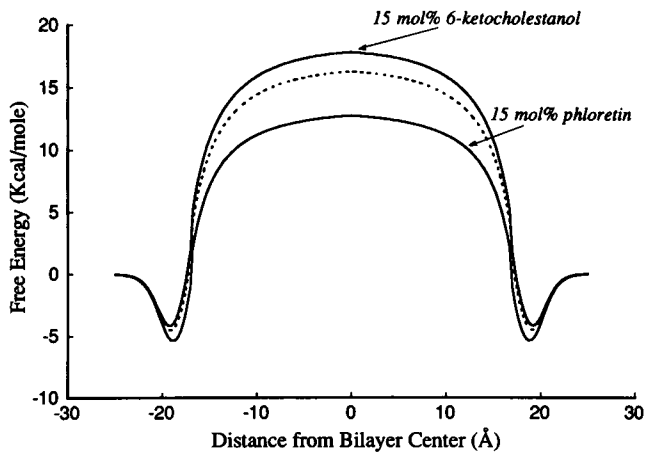

FIGURE 8 Calculated free energy profiles for probe I(8) in the presence of 15 mole% phloretin or 6-ketocholestanol. The dashed line represents the free energy profile for I(8) in unmodified egg PC membranes. These profiles were calculated using the point dipole model described under Experimental Procedures and parameters consistent with the data in Figs. 5 and 6. From these profiles, changes in the internal dipole potential in excess of 200 mV are possible by the addition of these compounds.

In conclusion, phloretin and 6-ketocholestanol were shown to modify both the binding and translocation rates of hydrophobic ions in lipid vesicle systems in a manner that is consistent with a lowering and raising of the internal dipole potential. A simple point dipole model used previously to examine the binding and translocation rates of ϕ_4P^+ and ϕ_4B^- was extended to include a wide range of hydrophobic ions. By incorporating an additional dipole layer into this model, it was possible to account for the binding and translocation rate changes produced by phloretin and 6-ketocholestanol. Thus, phloretin and 6-ketocholestanol appear to act by aligning in the interface such that their molecular dipole is aligned against or with the intrinsic dipole moment of the bilayer interface, respectively. The characterization of dipole potentials and agents that modify this potential in lipid vesicle systems provides a model system that can be used to study the electrostatic interactions between proteins and peptides with membranes.

This research was supported by a grant from the National Institutes of Health (GM-35125) to D. S. Cafiso.

J. C. Franklin received support from a National Institutes of Health training grant in molecular biophysics to the University of Virginia (GM08323).

REFERENCES

1. McLaughlin, S. A. 1989. The electrostatic properties of membranes. *Ann. Rev. Biophys. Biophys. Chem.* 18:113–136.
2. Mosior, M., and S. McLaughlin. 1991. Peptides that mimic the pseudosubstrate region of protein kinase C bind to acidic lipids in membranes. *Biophys. J.* 60:149–159.
3. Smaby, J. M., and H. L. Brockman. 1990. Surface dipole moments of lipids at the argon-water interface. Similarities among glycerol-ester-based lipids. *Biophys. J.* 58:195–204.

4. Liberman, E. A., and V. P. Topaly. 1969. Permeability of bimolecular phospholipid membranes for fat-soluble ions. *Biophysics*. 14:477–487.
5. LeBlanc, O. H. 1969. Tetraphenylborate conductance through lipid bilayer membranes. *Biochim. Biophys. Acta*. 193:350–360
6. Hladky, S. B. 1974. The energy barriers to ion transport by nonactin across thin lipid membranes. *Biochim. Biophys. Acta*. 352:71–85.
7. Andersen, O. S., and M. Fuchs. 1975. Potential energy barriers to ion transport within lipid bilayers. Studies with tetraphenylborate. *Biophys. J.* 15:795–830.
8. Pickar, A. D., and R. Benz. 1978. Transport of oppositely charged lipophilic probe ions in bilayer membranes having various structures. *J. Membr. Biol.* 44:353–376.
9. Hladky, S. B., and D. A. Haydon. 1983. Membrane conductances and surface potential. *Biochim. Biophys. Acta*. 318:464–468.
10. Flewelling, R. F., and W. L. Hubbell. 1986. The membrane dipole potential in a total membrane potential model. Applications to hydrophobic ion interactions with membranes. *Biophys. J.* 49:541–552.
11. Ellena, J. F., R. N. Dominey, S. J. Archer, Z-C. Zu, and D. S. Cafiso. 1987. The localization of hydrophobic ions in phospholipid bilayers using ^{1}H nuclear Overhauser effect spectroscopy. *Biochemistry*. 26: 4584–4592
12. Simon, S. A., and T. J. McIntosh. 1989. Magnitude of the solvation pressure depends on dipole potential. *Proc. Natl. Acad. Sci. USA*. 86: 9263–9267.
13. Gawrisch, K., D. Ruston, J. Zimmerberg, V. A. Parsegian, R. P. Rand, and N. Fuller. 1992. Membrane dipole potentials, hydration forces, and the ordering of water at membrane surfaces. *Biophys. J.* 61:1213–1223.
14. Sheng, C., and G. Vanderkooi. 1992. Molecular origin of the internal dipole potential in lipid bilayers: calculation of the electrostatic potential. *Biophys. J.* 63:935–941.
15. Cafiso, D. S. 1991. Lipid bilayers: membrane-protein electrostatic interactions. *Curr. Opin. Struct. Biol.* 1:185–190.
16. Dalbey, R. E. 1990. Positively charged residues are important determinants of membrane protein topology. *Trends Biochem. Sci.* 15:253–257.
17. McLaughlin, S., and J. Dilger. 1980. The transport of protons across membranes by weak acids. *Physiological Rev.* 60:825–863.
18. Flewelling, R. F., and W. L. Hubbell. 1986. Hydrophobic ion interactions with membranes. Thermodynamic analysis of tetraphenylphosphonium binding to vesicles. *Biophys. J.* 49:531–540.
19. Andersen, O. S., Finkelstein, A., Katz, I., and A. Cass. 1976. Effect of phloretin on the permeability of thin lipid membranes. *J. Gen. Physiol.* 67:749–771.
20. Melnik, E., Latorre, R., Hall, J., and D. Tosteson. 1977. Phloretin induced changes in ion transport across lipid bilayer membranes. *J. Gen. Physiol.* 69:243–257.
21. Reyes, J., Greco, F., Motais, R., and R. Latorre. 1983. Phloretin and phloretin analogues: mode of action in planar bilayers and monolayers. *J. Membr. Biol.* 72:93–103.
22. Perkins, W. R., and D. S. Cafiso. 1987. A procedure using voltage-sensitive spin-labels to monitor dipole potential changes in phospholipid vesicles: the estimation of phloretin-induced conductance changes in vesicles. *J. Membr. Biol.* 96:165–173.
23. Franklin, C., D. Cafiso, R. Flewelling, and W. Hubbell. 1993. Probes of membrane electrostatics. Synthesis and voltage-dependent partitioning of negative hydrophobic ion spin-labels in lipid vesicles. *Biophys. J.* 64:642–653.
24. Cafiso, D. S., and W. L. Hubbell. 1981. EPR determination of membrane potentials. *Annu. Rev. Biophys. Bioeng.* 10:217–244.
25. Simon, S. A., T. J. McIntosh, A. D. Magid, and D. Needham. 1992. Modulation of the interbilayer hydration pressure by the addition of dipoles at the hydrocarbon/water interface. *Biophys. J.* 61:786–799.
26. Singleton, W. S., Gray, M. S., Brown, M. L., and J. L. White. 1965. Chromatographically homogeneous lecithin from egg phospholipids. *J. Am. Oil. Chem. Soc.* 42:53–56.
27. Bartlett, G. R. 1959. Phosphorous assay in column chromatography. *J. Biol. Chem.* 243:466–468.
28. Cafiso, D. S., and W. L. Hubbell. 1982. Transmembrane electrical currents of spin-labeled hydrophobic ions. *Biophys. J.* 39:263–272.
29. Bechinger, B., and J. Seelig. 1991. Interaction of electric dipoles with phospholipid head groups. A H-2 and P-31 NMR study of phloretin and phloretin analogs in phosphatidylcholine membranes. *Biochemistry*. 30: 3923–3929.
30. Ketterer, B., B. Neumcke, and P. Lauger. 1971. Transport mechanism of hydrophobic ions through lipid bilayer membranes. *J. Membr. Biol.* 5:225–245.
31. McConnell, H. M. 1991. Structures and transitions in lipid monolayers at the air-water interface. *Annu. Rev. Physical Chem.* 42:171–195.
32. Ellena, J. F., S. J. Archer, R. N. Dominey, B. D. Hill, and D. S. Cafiso. 1988. Localizing the nitroxide group of fatty acid and voltage-sensitive spin-labels in phospholipid bilayers. *Biochim. Biophys. Acta*. 940:63–70.